

# Jamming in two-dimensional packings

Sam Meyer<sup>a</sup>, Chaoming Song<sup>b</sup>, Yuliang Jin<sup>b</sup>, Kun Wang<sup>b</sup>, Hernán A. Makse<sup>b,\*</sup>

<sup>a</sup>*École Normale Supérieure de Lyon, Université Claude Bernard, Lyon I, France 695014*

<sup>b</sup>*Levich Institute and Physics Department, City College of New York, New York, NY, USA 10031*

---

## Abstract

We investigate the existence of random close and random loose packing limits in two-dimensional packings of monodisperse hard disks. A statistical mechanics approach—based on several approximations to predict the probability distribution of volumes—suggests the existence of the limiting densities of the jammed packings according to their coordination number and compactivity. This result has implications for the understanding of disordered states in the disk packing problem as well as the existence of a putative glass transition in two dimensional systems.

*Keywords:* Random packings; Volume function; Disordered system

---

## 1. Introduction

The concept of jamming is a common feature of out of equilibrium systems experiencing a dynamical arrest ranging from emulsions, colloids, glasses and spin glasses, as well as granular materials [1]. For granular matter, it is argued that a statistical mechanical description can be used, with volume replacing energy as the conservative quantity [2]. In this framework, a mesoscopic model has been presented [3], allowing the development of a thermodynamics for jamming in any dimension. Here we develop this theoretical approach to investigate the existence of disordered packings in two-dimensional systems composed of equal-sized hard disks [4]. The existence of amorphous packings in 2d is a problem of debate in the literature: two dimensional systems are found to crystallize very easily since disordered packings of disks are particularly unstable [5].

In two dimensional Euclidean space, the hexagonal packing arrangement of circles (honeycomb circle packing) has the highest density of all possible plane packings (ordered or disordered) with a volume fraction  $\phi_{\text{hex}} = \frac{\pi}{\sqrt{12}} \simeq 0.9069$  and each disk surrounded by 6 disks. Regarding amorphous packings, experiments find a maximum density of random close packing (RCP) of monodisperse spheres at  $\phi_{\text{rcp}} \approx 0.82$  [4] while the lower limit (random loose packing, RLP) has

---

\*Corresponding author

Email address: [hmakse@lev.ccny.cuny.edu](mailto:hmakse@lev.ccny.cuny.edu) (Hernán A. Makse)

been little investigated and its existence has not been treated so far. The tendency of 2d packings to easily crystallize has led to consider bidisperse systems which pack at a higher RCP volume fractions of  $\phi_{\text{rcp}} \approx 0.84$  [6, 7].

In parallel to studies in the field of jamming—which consider the packing problem as a jamming transition approached from the solid phase [8, 6, 7]—other studies attempt to characterize jamming approaching the transition from the liquid phase [9, 10]. Here, amorphous jammed packings are seen as infinite pressure glassy states [9]. Therefore, the existence of disordered jammed structures (of frictionless particles) is related to the existence of a glass transition in 2d [9], a problem that has been debated recently [11].

Here we treat the disordered disk packing problem with the statistical mechanics of granular jammed matter [2]. The formal analogy with classical statistical mechanics is the following: the microcanonical ensemble, defined by all microstates with fixed energy, is replaced by the ensemble of all jammed microstates with fixed volume. Hence, the appropriate function for the description of the system is no longer the Hamiltonian, but the *volume function*,  $\mathcal{W}_i$ , giving the volume available to each particle unit such that the total system volume is  $V = \sum_i \mathcal{W}_i$  [2].

The aim of the present work is to develop the model presented in [3] for the calculation of the volume function in the case of 2d packings. The validity of the hypothesis employed in [3] are discussed, and they are modified according to the properties of 2d packings. We use our results to study the nature of the RLP and RCP limit in 2d through an elementary construction of a statistical mechanics that allows the study of the existence of a maximum and minimum attainable density of disordered circle packings. We find that amorphous packings can pack between the density limits of  $\sim 77.5\%$  and  $\sim 80.6\%$  defining the RLP and RCP respectively, according to system coordination number and friction, opening such predictions to experimental and computational investigation. While these values should be considered as bounds to the real values due to the approximations used in the theory, they serve to suggest the existence of both limits in two dimensional packings of monodisperse disks.

It should be noted that this theoretical model is developed for disordered packings, and RLP and RCP represent two well defined bounds in the model under isostatic conjecture. However, the nature of RCP in 2d is still not clear. A recent study [12] has shown that partially crystallized jammed packings exist in 3d and RCP could be interpreted as the “freezing point” in a first-order phase transition between ordered and disordered packing phases. It is possible that a similar first-order phase transition exists in 2d as well [13, 14], or that there is a continuous variation at RCP, since crystallization of two dimensional systems can be easily achieved. Beyond the pure amorphous packings, crystallized states should be taken into account and future work is still required to complete the picture in 2d.

## 2. Volume function

The volume function is the key of the system's statistics: its flat average over all jammed configurations determines the total volume. The most natural way of dividing the system is called the Voronoi diagram, which can be seen in Fig. 1a. Each grain's region is the part of the space closer to this grain than to any other, so that the volume is clearly additively partitioned. The major drawback of this construction is that, so far, there was no analytical formula for the Voronoi volume of each cell, such that attempts have been made to use other constructions [15].

The Voronoi volume of a particle  $i$  can be written as:

$$\mathcal{W}_i^{\text{vor}} = \frac{1}{2} \oint \left( \min_{\hat{s} \cdot \hat{r}_{ij} > 0} \frac{r_{ij}}{2\hat{s} \cdot \hat{r}_{ij}} \right)^2 ds, \quad (1)$$

where  $\vec{r}_{ij}$  is the vector from the position of particle  $i$  to  $j$ , the average is over all the directions  $\hat{s}$  forming an angle  $\theta_{ij}$  with  $\vec{r}_{ij}$  as in Fig. 1a. This formula has a simple interpretation depicted in Fig. 1a. For consistency of notation with previous work, we will use the words "volume" and "surface" in 2d, although they correspond to "surface" and "length" respectively.

The volume function defined in terms of the particle coordinates is of no use, since it does not permit the calculation of the partition function. To solve this problem, we calculate an average free volume function based on the environment of the particle, referring to a coarse-graining over a certain mesoscopic length scale. We assume a probability distribution for the positions of the nearest neighbors as well as the other particles. After averaging over the probability distribution we obtain an average mesoscopic free volume function representing quasiparticles in the partition function. Considering isotropic amorphous packings allows for removal of the orientational averaging.

## 3. Probability distribution of volumes

Using the notation of Fig. 1b, we see that the microscopic volume function is entirely defined by the parameter  $c = \min[r/\cos\theta]$ . The calculation of the average free volume function,  $w$ , requires knowledge of the probability distribution of this parameter. That is:

$$w \equiv \langle \mathcal{W}_i^{\text{vor}} \rangle / V_g - 1 = - \int_{c=1}^{\infty} (c^2 - 1) \frac{dP_>}{dc} dc, \quad (2)$$

where  $P_>(c)$  represents the inverse cumulative distribution, i.e. the probability that all balls verify  $r_{ij}/\cos\theta_{ij} > c$ , which is calculated under the following hypothesis:

(1) The cumulative distribution  $P_>(c)$  is made of two contributions, one of the "contact" balls (*i.e.* touching the considered grain), called  $P_>^C$ , and one of the other (background) balls,  $P_>^B$ . These probabilities can be understood as the probabilities of a particle in contact (resp. background) for being situated

outside the grey zone on Fig. 1b, and therefore not contributing to the Voronoi volume  $c^2$ .

(2) The probability distributions are those of a large number of particles at a given density, and of negligible size giving rise to Boltzmann-like distributions:

$$P_>^B(c) = \exp(-\rho V^*(c))$$

and

$$P_>^C(c) = \exp(-\rho_S S^*(c)).$$

Here  $V^*$  and  $S^*$  represent a free volume and surface respectively towards  $c$ , *i.e.*  $V^*(c) = \int \Theta(c - \frac{r}{\hat{r} \cdot \hat{s}}) d\bar{r}$  and  $S^*(c) = \oint \Theta(c - \frac{1}{\hat{r} \cdot \hat{s}}) ds$  where the integrals cover respectively the space and the unity sphere. The densities,  $\rho(w)$  and  $\rho_S(z)$ , are mean free-volume and free-surface densities, respectively.

In 2d, the volume of the grain (with  $2R = 1$ ) is  $V_g = \pi/4$ . The free volume density (inverse of the free volume per particle) is  $\rho(w) = N/(NV_g\phi^{-1} - NV_g) = 1/(V_g w)$ . Then,

$$V^*(c) = \left[ \frac{c^2}{2} - 1 \right] \arccos(1/c) + \frac{c}{2} \sqrt{1 - \frac{1}{c^2}}.$$

The main assumption here is that the packing structure is uniform, thus the pair distribution function is assumed to be a delta function at contact plus a constant for larger distances. This assumption is an oversimplification, and more realistic background could be considered, such as peaks in the pair distribution at the next nearest neighbor sites.

For the surface contribution, we have:

$$S^*(c) = 2 \int_0^{\arccos(1/c)} d\theta = 2 \arccos(1/c).$$

The surface density  $\rho_S = 1/\langle S \rangle$  is the inverse of the average surface left free by  $z$  contact balls (see Fig. 2a). As a rough approximation, one can assume it is proportional to  $z$ , but because of the size of one ball, there is an "excluded-surface" effect, so that the exact value is determined by numerical simulations. It consists in setting sequentially and randomly  $z$  non-overlapping circles of radius 1 at the surface of the unity circle (Fig. 2a). The closest ball to the considered direction  $\hat{s}$  defines the free angle. The free surface is then twice this angle. Its average value is the mean free-surface  $\langle S \rangle$ .

Results are shown in Fig. 2b. Important deviations from the linearity in  $z$  are not surprising, since each contact ball occupies an important surface ( $z_{max} = 6$  in 2d), and strong finite-surface effects are expected. For  $z = 5$ , in around 41% of the trials, the fifth ball cannot be set because there is not enough space, and we take into account only the 59% remaining trials.

For  $3 \leq z \leq 4$ , we will use the linear dependency  $\rho_S(z) = \frac{z-0.5}{\pi}$  as fitted in Fig. 2. Obviously a fitting for  $1 \leq z \leq 5$  would be of higher order, but in our range, the error is insignificant compared to other approximations of the model.

(3) The cumulative distributions are not independent. The assumption that the surface and volume terms do not overlap seems to be an abusive approximation in 2d. This is not the case in 3d as shown in [3]. Indeed, for higher dimensions the probabilities are expected to become independent, but in the case of 2d a new solution has to be worked out which considers the correlations between the contact and background term.

To illustrate this point, Fig. 3a shows the considered grain, the free volume  $V^*(c)$  and the circle occupied by the closest "contact-grain" (*i.e.* the excluded zone for the center of any other grain because of its presence) for a value of  $c = 1.2$ . In fact, the values of  $c < 1.2$  are contributing for 94% of the distribution if we neglect the overlap of contact and background grains. As we see, the free volume is mostly covered up by this contact-grain, and the non-overlapping hypothesis used in [3] appears obviously wrong. This statement is confirmed by the calculation of the RCP density: with the non-overlapping hypothesis, the calculation provides a value of  $\phi_{RCP} = 0.89$ , to be compared with the reported value of 0.82. The nearer grains are exceedingly taken into account.

Therefore, the volume term is modified by substituting the free volume  $V^*$  by  $V^* - \Delta V^*$  which represents the free volume minus the part occupied by the closest surface grain. The meaning of this change is that the contributions are no longer independent, and depend on two parameters  $c_B$  and  $c_C$ . The distribution  $P_>(c)$  is the probability that both  $c_C$  and  $c_B$  be higher than  $c$ . Figure 3b shows the overlap of the contact grain parameterized by  $c_C$  and the background volume parameterized by  $c_B$ , defining  $\Delta V^*(c_B, c_C)$ . The analytical formula of  $\Delta V^*$  is determined by geometrical calculations.

The probability density is

$$P(c) = -dP_>/dc = -P_>^C(c) \cdot dP_>^B/dc - P_>^B(c) \cdot dP_>^C/dc.$$

The meaning of the latter equality is that, to realize  $c$ , we must have either  $c_C$  or  $c_B$  equal to  $c$ , and the other higher. The background probability depends on  $c_C$ :

$$P_>^B(c_B|c_C) = \exp[-\rho(V^*(c_B) - \Delta V^*(c_B, c_C))],$$

and

$$P^B(c_B|c_C) = -\frac{d}{dc_B}P_>^B(c_B|c_C).$$

Then,

$$\begin{aligned} P(c) &= \int_{c_C=c}^{\infty} P^C(c_C)P^B(c|c_C)dc_C + P^C(c)P_>^B(c|c) = \\ &= -\frac{d}{dc} \int_{c_C=c}^{\infty} P^C(c_C)P_>^B(c|c_C)dc_C = -\frac{d}{dc}P_>(c). \end{aligned}$$

From (2), we integrate by parts using the latter equality. The boundary term  $[(c^2 - 1)P_>(c)]$  vanishes, since the limits of integration correspond to  $c = 1$  and  $c \rightarrow \infty$ , with  $P(c \rightarrow \infty) = 0$ . We obtain for the average volume function

from Eq. (2):

$$w = 2 \int_{c=1}^{\infty} c \int_c^{\infty} \frac{dP_>^C}{dc_C} \exp[-\rho(w)(V^*(c) - \Delta V^*(c, c_C))] dc_C dc \quad (3)$$

with  $P_>^C(c_C) = \exp[-\rho_S(z)S^*(c_C)]$ .

#### 4. Free volume function

Equation (3) is a self-consistent equation to obtain  $w(z)$ , which cannot be solved exactly, therefore a numerical integration of (3) is necessary to obtain  $w$  vs  $z$ . For various values of  $z$ , we integrate Eq. (3) numerically, and we then calculate a fitting of the results (Fig. 4a). We obtain the free volume function and the local density  $\phi_i^{-1} = w + 1$  (Fig. 4b):

$$w(z) = 0.437 - 0.049z, \quad \phi_i(z) = \frac{1}{1.437 - 0.049z}. \quad (4)$$

Generally speaking, we would expect  $w$  to be roughly proportional to  $1/z$ , with  $w \rightarrow 0$  when  $z \rightarrow \infty$ . However, the statement  $z \rightarrow \infty$  has little meaning when we plot a figure for  $3 < z < 4$  and the "infinite" (maximal) value of  $z$  is 6.

#### 5. Statistical mechanics

Equation (4) plays the role of a "Hamiltonian" of the system. Each jammed configuration corresponds to some "volume level" in analogy with energy levels in Hamiltonian systems. From the formal analogy with classical formulas, the canonical partition function is [2]:

$$\mathcal{Z}(Z, X) = \int g(w) e^{-w/X} dw, \quad (5)$$

where  $X$  is the (reduced) compactivity (normalized by the volume of the spheres) and  $g(w)$  is density of states for a given volume  $w$ . We remind that the compactivity is the equivalent of temperature in the Edwards statistics, and it is a measure of the system's looseness.

Since the volume  $w$  is now directly related to coordination number  $z$  through Eq. (4), we can compute  $g(w)$  by replacing variable,  $g(w) = \int P(w|z)g(z)dz$ , where  $P(w|z)$  is the conditional probability and  $g(z)$  is the density of states for given  $z$  [3].

At this point a distinction has to be emphasized: we refer to  $z$  as the geometrical coordination number since it is purely defined by the particle positions. On the other hand, there is the mechanical coordination number,  $Z$ , defined by those geometrical contacts that carry a non-zero force.  $Z$  is then defined by the mechanical constraint leading to the isostatic condition. A packing is isostatic when the number of contact forces equals the number of force and torque balance equations [3]. For example, for a packing of  $N$  infinitely rough particles

in  $d$  dimensions, each mechanical contact carries one normal force and  $d - 1$  tangential force components, and for each particle there are  $d$  force balance equations and  $\frac{1}{2}d(d - 1)$  torque balance equations. The isostatic condition requires that  $\frac{1}{2}dNZ = dN + \frac{1}{2}d(d - 1)N$ , or  $Z = d + 1$ . On the other hand, for frictionless packings, frictional forces or tangential forces do not exist and the torque balance equations are not taken into account. The isostatic condition in this case leads to the relation  $Z = 2d$ . For a system with a finite interparticle friction  $\mu$ ,  $Z(\mu)$  interpolates between both limits [7, 3]. It should be noted that the above calculations of the isostatic condition are based on the mechanical coordination number  $Z$ , rather than the geometrical coordination number  $z$ , because a geometrical contact does not necessarily provide a mechanical constraint. For instance, two particles are free to rotate with respect to each other if the contact between them is geometrical and does not carry any tangential forces.

Obviously,  $z$  must be larger than  $Z$  for the mechanical condition to be satisfied. The different volume levels of a packing can be understood in the following way: the friction coefficient sets a mechanical constraint on  $Z$ , but the system can explore all geometrical levels  $z > Z$ . Additionally,  $z$  is bounded by the maximal coordination number for a random packing, which is  $2d = 4$ , since there are  $z/2$  constraints on the  $d$  particle coordinates. In relation with the discussion of isostaticity, it is believed that above this value, the system is partially crystallized. Therefore we obtain:  $g(w) = \int_Z^4 P(w|z)g(z)dz$ . Since  $w(z)$  from Eq. (4) is a coarse-grained free volume and independent of the microscopic positions of particles, we have  $P(w|z) = \delta(w - w(z))$ .

The expression of the density of states is obtained by considering that the states are collectively jammed. Therefore, the space of configuration is discrete since we cannot continuously obtain one configuration from another. Assuming a typical distance between configurations as  $h_z$ , we obtain  $g(z) \propto (h_z)^z$ , the exponent  $z$  arising since there are  $z$  position constraints per particle in the jammed state compared to the free (gas) state. Such a formula is analogous to the factor  $h^{-d}$  for the density of states in traditional statistical mechanics, where  $h$  is the Planck constant, which arises because of the uncertainty principle, *i.e.* because of the discreteness of the elementary volume of phase space.

Substituting into Eq. (5), we get :

$$\mathcal{Z}(Z, X) = \int_Z^4 (h_z)^z e^{-w(z)/X} dz \quad (6)$$

To establish the maximum and minimum densities, we consider the limits of zero and infinite compactivity, respectively. The ground state of jammed matter, is analogous with the limit  $T \rightarrow 0$ . The only accessible state is  $z = 4$ , corresponding to the random close packing. For this state, from Eq. (4) we get a fixed value of the volume fraction for any coordination number  $Z \in [3, 4]$ ,  $\mu \in [0, \infty]$ :

$$\phi_{rcp}(Z) = \frac{1}{1.437 - 0.049 \times 4} \approx 0.806, \quad (7)$$

The lower density appears for  $X \rightarrow \infty$  when the Boltzmann factor is unity in Eq. (6), and we obtain the densities of RLP (assuming  $h_z \ll 1$ ):

$$\begin{aligned}\phi_{rlp}(Z) &= \frac{1}{Z(Z, \infty)} \int_Z^4 \frac{1}{1.437 - 0.049z} (h_z)^z dz \approx \\ &\approx \frac{1}{1.437 - 0.049Z}, \quad Z \in [3, 4].\end{aligned}\quad (8)$$

This leads to the diagram in the plane  $(\phi, Z)$  plotted in Fig. 4c defining the possible jammed configurations. On the right part of the vertical line defined by Eq. (7), no disordered packing can exist. To the left of Eq. (8), the packings are not mechanically stable.

Between these two lines, we plot the lines of constant finite compactivity. For a finite value of the compactivity, the equation  $\phi(Z)$  is calculated by numerical integration. In the figure, three curves are plotted, respectively  $X = 5.10^{-3}$ ,  $X = 10^{-2}$  and  $X = 10^{-1}$  for  $h_z = 0.01$ . The compactivity increases from the right ( $X = 0$ ) to the left ( $X \rightarrow \infty$ ). The limit  $\mu \rightarrow \infty$ ,  $Z \rightarrow 3$  defines the lowest RLP density value which is predicted:

$$\phi_{rlp}^{\min} = \phi_{rlp}(Z = 3) = \frac{1}{1.437 - 0.049 \times 3} \approx 0.775 \quad (9)$$

The value of  $\phi_{rlp}$  depends on the mechanical coordination number, contrarily to the value of  $\phi_{rcp}$ . The shape of the diagram is similar in 3d [3], and this is in agreement with the wide range of reported values for RLP, in contrast with RCP [4]. On a horizontal line given by a system with fixed  $Z$ , packings of different volume fractions can be achieved by applying different quench rates or compression speeds during the preparation protocol. Slow compressions achieve loose packings (and high compactivities). The obtained predictions for the density of RCP are close to the experimental values while we predict the existence of a RLP density.

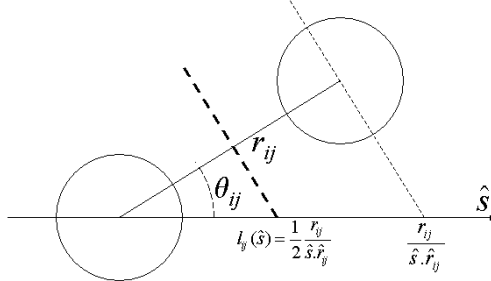
## 6. Summary

In summary, we have used a model of volume fluctuations to develop a statistical mechanics of granular matter in 2d. From a quantitative point of view, we have seen how it lies on several approximations, that can appear too rough. The main difference with the 3d case is the need of taking into account properly the correlations in the probability distribution of volume through the consideration of point (3) above. Indeed, if we take  $P_C^C$  and  $P_B^B$  to be independent as considered in [3] we find  $\phi_{rlp} = 0.84$  and  $\phi_{rcp} = 0.89$ , both values above the experimental value of RCP. The results, although not allowing exact predictions, are situated in the right order of magnitude for the limiting volume fractions. Due to the several approximations of the theory, the resulting limiting densities have to be considered as bounds to the real values. Improvements can be achieved by taking into account the size and shape of the disks, as well as exact

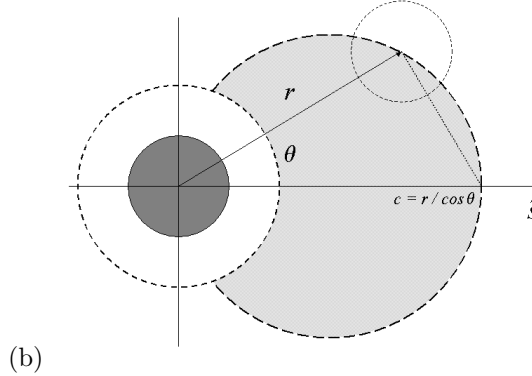
enumeration to calculate  $P_{>}(c)$ , which can be done at least to a prescribed coordination shell of particles, in a brute force analysis analogous to the Hales proof of the Kepler conjecture, currently being undertaken. Altogether, the present framework seems to be successful in describing at least qualitatively the general features of jammed granular matter in 2d providing evidence of the existence of RCP and RLP and their density value. These results suggest that a putative ideal glass transition may also exist in frictionless hard disk as discussed in [9].

## References

- [1] A. Coniglio, A. Fiero, H. J. Herrmann, M. Nicodemi eds. *Unifying Concepts in Granular Media and Glasses* (Elsevier, Amsterdam, 2004).
- [2] S. F. Edwards and R. B. S. Oakeshott, Physica A **157** 1080 (1989).
- [3] C. Song, P. Wang, and H. A. Makse, Nature **453**, 629 (2008).
- [4] J. G. Berryman, Phys. Rev. A **27**, 1053 (1983).
- [5] C. Brito and M. Wyart, Europhys. Lett. **76**, 149 (2006).
- [6] C. S. O'Hern, S. A. Langer, A. J. Liu and S. R. Nagel, Phys. Rev. Lett. **86**, 111 (2002).
- [7] T. Unger, J. Kertész, and D. E. Wolf, Phys. Rev. Lett. **94**, 178001 (2005).
- [8] H. A. Makse, D. L. Johnson and L. M. Schwartz, Phys. Rev. Lett. **84**, 4160 (2000).
- [9] G. Parisi, and F. Zamponi, J. Chem. Phys. **123**, 144501 (2005); arXiv:cond-mat/08022180
- [10] B. D. Lubachevsky and F. H. Stillinger, J. Stat. Phys. **60**, 561 (1990); M. Skoge, A. Donev, F. H. Stillinger, and S. Torquato, Phys. Rev. E **74**, 041127 (2006).
- [11] Y. Brumer and D. Reichman, J. Phys. Chem. B **108**, 6831 (2004); A. Donev, F. H. Stillinger, and S. Torquato Phys. Rev. Lett. **96**, 225502 (2006); M. Tarzia, J. Stat. Mech.: Theory and Experiment, P01010 (2007).
- [12] Y. Jin and H. A. Makse (2010), arXiv:1001.5287v1 [cond-mat.soft].
- [13] M. D. Shattuck (2006), arXiv:cond-mat/0610839v1 [cond-mat.soft].
- [14] D. Aristoff and C. Radin (2009), arXiv:0909.2608v1 [cond-mat.soft].
- [15] R. C. Ball and R. Blumenfeld, Phys. Rev. Lett. **88**, 115505 (2002).

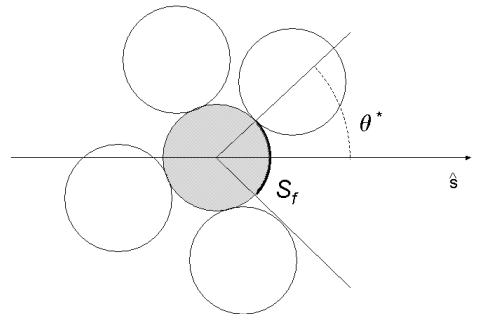


(a)

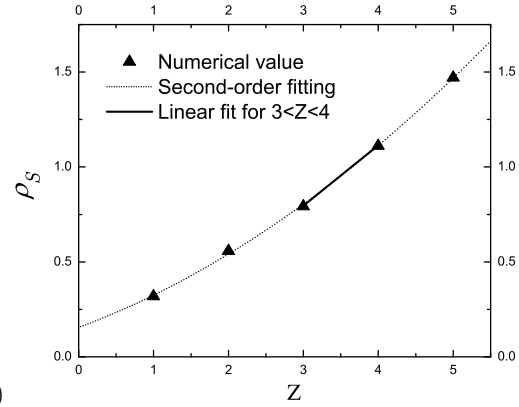


(b)

Figure 1: (a) The limit of the Voronoi cell of particle  $i$  in the direction  $\hat{s}$  is  $r_{ij}/2 \cos \theta_{ij}$ . Then the Voronoi volume is proportional to the integration of  $(r_{ij}/2 \cos \theta_{ij})^2$  over  $\hat{s}$  as in Eq. (1). (b) The particle contributing to the Voronoi volume along  $\hat{s}$  is located at  $(r, \theta)$ . The dark gray region is the considered grain ( $r < R$ ), and in white the excluded zone for the center of any other grain ( $r < 2R$ ). For a given  $c = r / \cos \theta$ , the light gray area is the region of the plane  $(r', \theta')$  where  $r'/\cos\theta' < c$ .



(a)



(b)

Figure 2: (a) Free surface, in an example of  $z = 4$  contact balls, defined by the angle of the closest grain to  $\hat{s}$ , with  $\langle S \rangle = 2\theta^*$ . (b) Simulation results for  $1 \leq z \leq 5$ , with a second-order polynomial fitting, and linear fitting for  $3 \leq z \leq 4$  :  $\rho_S = (z - 0.5)/\pi$

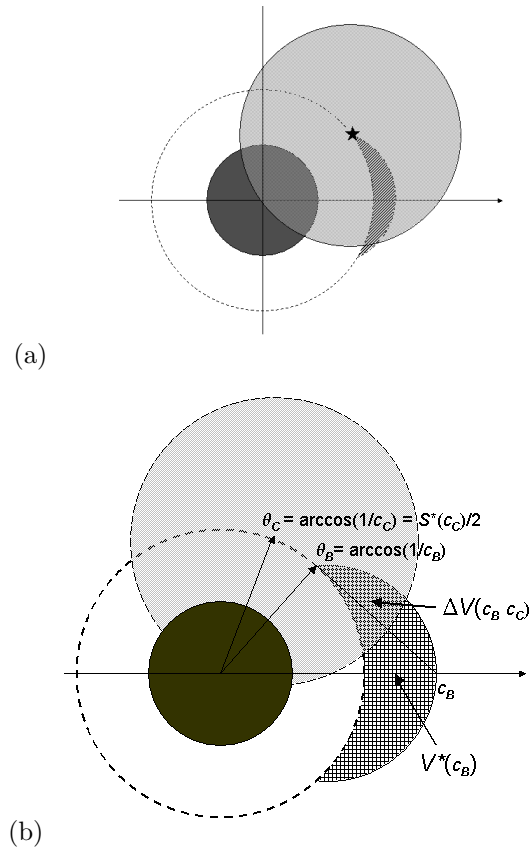


Figure 3: (a) For  $c = 1.2$ , the star is the center of the closest contact-grain, occupying the circular region printed with a pattern. The free volume is printed in grey. It is almost completely overlapped by the surface contribution. (b) The closest contact-ball depends on  $c_C$ , the free volume on  $c_B$ , and  $\Delta V$  on both. Here it is the intersection between the region in light grey and the patterned region.

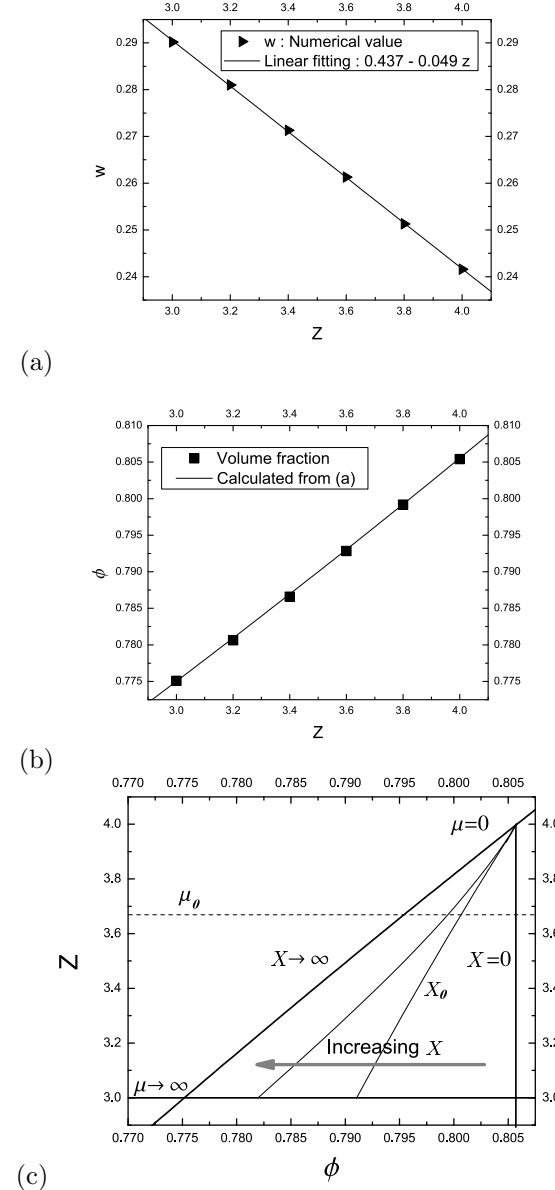


Figure 4: (a)  $w(z)$  curve, with a linear fitting:  $w(z) = 0.437 - 0.049z$ . (b) Volume fraction according to the second Eq. (4). (c) Prediction of the model. The thick curves are the limit of the diagram at  $X = 0$  and  $X \rightarrow \infty$ . We show several curves of constant compactivity,  $X$ . The curves are plotted for (from right to left) :  $X = 5 \cdot 10^{-3}$ ,  $X = 10^{-2}$  and  $X = 10^{-1}$ . The horizontal lines are both constant  $Z$  given by an arbitrary  $\mu_0$  (dotted) and  $\mu \rightarrow \infty$  (thick inferior limit of the diagram).